Optically nonlinear effects in intersubband transitions of GaN/AlN-based superlattice structures

Daniel Hofstetter,[a] Esther Baumann, and Fabrizio R. Giorgetta
Institute of Physics, University of Neuchatel, 1 A.-L. Breguet CH-2000, Neuchatel, Switzerland
Fabien Guillot, Sylvain Leconte, and Eva Monroy
Equipe Mixte CEA-CNRS-UJF Nanophysique et Semiconducteurs, DRFMC/SP2M/PSC, CEA-Grenoble, 38054 Grenoble Cedex 9, France

We report optically nonlinear processes related to near-infrared intersubband transitions in short period GaN/AlN superlattices. The strong piezo- and pyroelectric effects in this material lead to intrinsic asymmetries in the electronic potential of the superlattice, and thus to strong nonlinearities of the optical susceptibility. Because of the large intersubband transition energy of nearly 1 eV and the short lifetime of excited electrons in the upper quantum state, these nonlinear effects can be exploited for the fabrication of room temperature operated high-frequency detectors in the telecommunication wavelength range. At the same time, saturation effects due to resonant two-photon absorption could be observed.

Nonlinear optical (NLO) materials are exploited in versatile tunable laser sources for spectroscopy and optical pump-probe measurements,[1] and have recently made their way into everyday applications such as the green laser pointer.[2] Due to the nonlinear dependence of their electrical polarization on an electromagnetic field, such materials are capable of converting incoming light into radiation at multiples of the input frequency. In the early days of nonlinear optics, mainly naturally occurring materials such as Potassium hydrogen phosphate (KH_2PO_4), Lithium niobate ($LiNbO_3$), or Potassium phosphate (KPO_3) were used to expand the limited spectral regime of laser light sources by optical frequency doubling,[3] difference frequency generation, and optical rectification (OR).[4] In 1989, Rosencher *et al.* developed artificial NLO materials based on intersubband transitions in semiconductor quantum structures,[5] in which the required noncentrosymmetric electronic potential was produced by carefully designed asymmetric quantum wells (QWs).[6] In their experiments, Rosencher *et al.* observed a large dc polarization under excitation with an ac electromagnetic field, which they called OR—in analogy to the classical NLO materials. For simplicity, we will be using the generic term OR to address both "classical OR" in NLO materials and a more generalized kind of "resonant OR" or "intersubband polarization" that takes place in QW-based structures. Owing to the relatively narrow bandgap of the semiconductors available at the time, all early OR experiments had to be performed in the midinfrared spectral region and required cryogenic cooling. Here, we address the potential of intersubband transitions in GaN/AlN nanostructures in terms of their NLO behavior. Thanks to the large conduction band offset of nearly 2 eV and the short electron lifetime in the upper quantum state, these materials show strong NLO effects in the technologically important wavelength range around 1.55 μm. Furthermore, due to the strong quantum confinement present in these materials, room-temperature observation of these effects becomes possible. After the first demonstration of intersubband absorption[7–9] and detection[10,11] in GaN/AlN-based nanostructures, the exact understanding of the detection mechanism in such components, as reported in this article, is a major breakthrough toward a practical application of GaN as NLO material in future high-speed optical telecommunication systems.

Unlike the more sophisticated steplike QW structures used by Rosencher *et al.* in 1989 and presented in Figs. 1(a) and 1(b), the GaN/AlN material system offers the required asymmetric QWs naturally, due to strong, internal piezo- and pyroelectric fields [see Fig. 1(c)]. In a first experiment, we have grown GaN/AlN superlattices with 40 periods and varied the GaN QW thickness (t_{well}=1.5, 2, 2.5, 3, and 3.5 nm) while keeping the AlN barrier thickness constant at 5 nm. Absorption spectra were measured under illumination with TM polarized light and in 45° multipass waveguide geometry. By changing the thickness of the QW from 1.5 to 3.5 nm, the intersubband absorption could be tuned from 6000 to 4900 cm^{-1}. For all of those samples, we observed more than one optical transition which can be explained by the naturally asymmetric shape of GaN-based QWs.

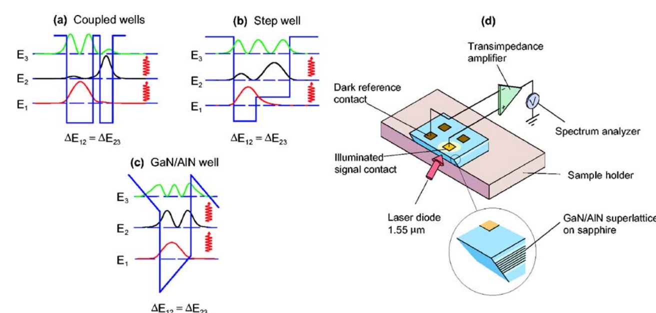

FIG. 1. (Color online) Schematic conduction band diagram of (a) steplike, (b) coupled, and (c) asymmetric GaN-based QWs. In all structures, double resonance between E_1, E_2, and E_3 is drawn. (d) Schematic representation of the detector. The blowup at the bottom shows the position of the superlattice active region with respect to the sample surface.

[a]Electronic mail: daniel.hofstetter@unine.ch

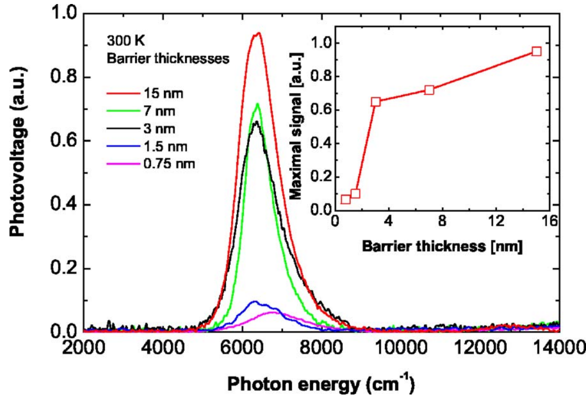

FIG. 2. (Color online) Dependence of the measured spectral photovoltage response as a function of barrier thickness. The inset shows the photovoltaic detector signal as a function of barrier thickness.

Following the epitaxial growth of the superlattices, entirely planar photodetector devices were fabricated by evaporation of two Ti/Au contacts on the sample surface. As schematically represented in Fig. 1(d), optical response spectra were obtained by illumination of one of the contacts through a single 45° facet, while the other contact remained dark. The resulting photovoltage is amplified and fed into the external detector port of a Fourier transform infrared spectrometer. In order to assess the detrimental effects of resonant tunneling in the photodetector operation, we have investigated a second series of samples with 1.5 nm GaN QWs and various AlN barrier thicknesses (t_{barrier}=0.75, 1.5, 3, 7, and 15 nm). As Fig. 2 shows, the detector performance improves with thicker AlN barriers, which demonstrates that resonant tunneling processes degrade the device performance when not properly designed in.

Preliminary assessment of high-frequency capabilities has been performed by exciting the devices with a modulated diode laser beam at 1.55 μm. The voltage response is amplified by a voltage amplifier and measured in a spectrum analyzer. The highest frequency for which we observed a signal is 2.937 GHz (see Fig. 3). Since the device design and packaging do not yet involve any impedance matching or parasitic capacitance reduction, a substantial improvement is expected in future optimized experiments of this type.

All of the above experimental observations can be understood on the basis of NLO effects as described in the

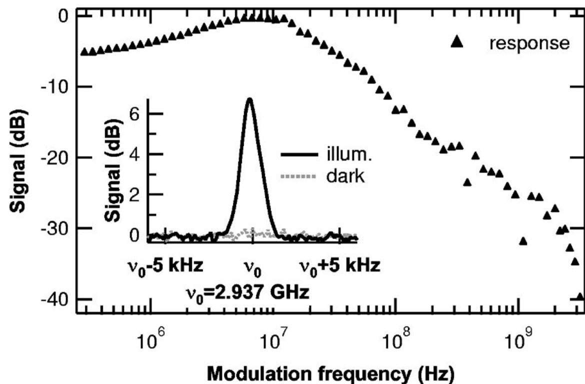

FIG. 3. Frequency response of a GaN/AlN-based detector showing a low-pass filter characteristics with a 3 dB frequency of 50 MHz. The steep signal drop at 2 GHz is due to the roll-off of the amplifier. The inset shows the signal measured under illuminated (black) and dark (light gray) conditions at the highest modulation frequency, i.e., at 2.937 GHz.

introduction. In contrast to quantum structures in nonpolar semiconductors, GaN/AlN QWs offer a natural, strong intrinsic asymmetry of the electronic potential due to their spontaneous and piezoelectric polarization fields.[12] Indeed, the potential well shape and the envelope functions of the bound states in a nitride-based well look very similar to the configuration in a steplike QW fabricated from nonpolar GaAs/AlGaAs. Since in a GaN/AlN superlattice, the excitation of an electron into the upper quantized level is accompanied by a small displacement in the growth direction [i.e., a lateral displacement in Fig. 1(c)], an electrical dipole moment is created.[13] For a high electron density and many QWs, these microscopic dipole moments add up to a macroscopic polarization of the crystal, which can be detected as an external photovoltage. This mechanism is known as resonant OR. Since for a certain well thickness, the energy of the optical transition between E_1 and E_2 happens to be exactly the same as between E_2 and E_4, we have, in addition, a situation referred to as "double-resonance," which enables second harmonic generation and other related two photon processes. In a semiconductor system like GaAs/AlGaAs, equidistant electronic levels can only be achieved by very sophisticated band-engineering techniques such as step QWs or coupled double QWs. In the GaN/AlN material system, however, double resonance occurs spontaneously because of the internal polarization induced widening of the uppermost region in each QW. According to the theory presented in Ref. 13, the maximal photovoltage on the device can be expressed via

$$V = \frac{q\delta_{12}}{\varepsilon_0\varepsilon_{\text{stat}}}\frac{I_{\text{in}}\tau_{\text{life}}}{\hbar\omega_{12}}\left[\frac{q^2\hbar}{2\varepsilon_0 ncm^*}\frac{f_{12}}{\gamma_{12}}n_s\frac{\sin^2\theta}{\cos\theta}N\right], \quad (1)$$

where $I_{\text{in}}=6\times10^7$ W/m^2 is the input intensity, N=400 is the number of active region periods (including the number of 10 passes), $\varepsilon_{\text{stat}}$=10.2 is the static dielectric constant of GaN, c is the speed of light, $m^*=0.2m_e$ is the GaN effective mass, θ=37° is the angle of incidence toward the surface normal, $n_s=1.5\times10^{13}$ cm^{-2} is the sheet carrier density, and finally δ_{12}=1.7 Å, γ_{12}=40 meV, f_{12}=0.7, $\omega_{12}=2\times10^{14}$ Hz, τ_{life} =370 fs are the mean electron displacement, half width at half maximum, oscillator strength, frequency, and upper state lifetime of the involved transition, respectively. For this set of parameters, we obtain a photovoltage of 140 μV/W, in good agreement with the experimental value of 130 μV/W at 150 K.

We have further investigated the nonlinear behavior of such GaN/AlN superlattices in terms of two-photon absorption/detection. For this purpose, the sample was illuminated either by a white light source or by a 1.55 μm single-mode laser diode. As described above, electrons excited into the E_2 level lead to OR. However, a small fraction of those excited electrons undergo further excitation from level E_2 into level E_4, leading to a noncoherent, resonant two-photon process. Because of the $E_2 \rightarrow E_4$ process, level E_2 "loses" electrons into level E_4. The probability for this process to happen can be expressed as

$$\eta = \frac{I_{\text{in}}\tau_{\text{life}}}{\hbar\omega_{12}}\left(\frac{q^2\hbar}{2\varepsilon_0 ncm^*}\right)^2\frac{f_{12}}{\gamma_{12}}\frac{f_{24}}{\gamma_{24}}n_s\frac{\sin^4\theta}{\cos\theta}N^2, \quad (2)$$

where all quantities are defined analogously to Eq. (1). In addition, f_{24}=0.4 is the oscillator strength and γ_{24}=40 meV is the half width at half maximum of the E_2 E_4 transition.

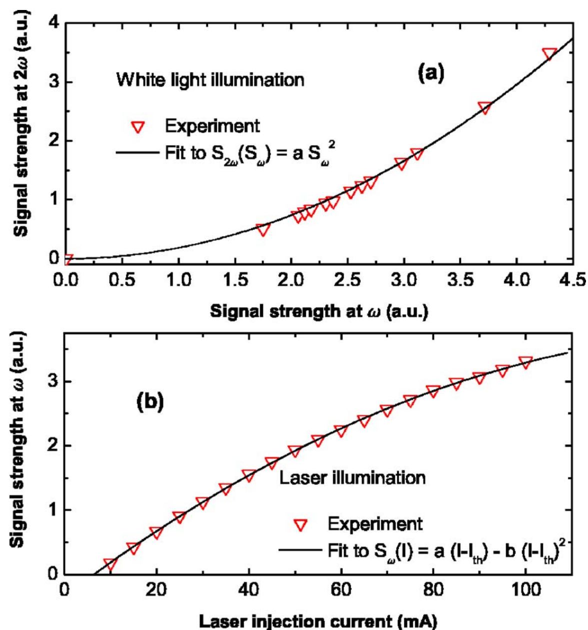

FIG. 4. (Color online) (a) Integrated signal strength (100 times) of the second harmonic frequency signal $S_{2\omega}$ as a function of the fundamental frequency signal S_ω using white light illumination. The triangular symbols correspond to the measured data points, while the line is a fit to the equation $S_{2\omega}(S_\omega)=aS_\omega^2$. (b) Integrated signal strength of the fundamental frequency signal S_ω as a function of laser injection current I. The symbols represent measured data points, whereas the line is a fit to the function $S_\omega(I)=a(I-I_{\rm th})\text{-}b(I-I_{\rm th})^2$.

Due to this process, the photovoltage of the $E_1 \rightarrow E_2$ transition experiences a deviation from linearity. For small input intensities, the size of the signal related to the normal $E_1 \rightarrow E_2$ process grows nearly linearly with incident intensity, whereas the $E_1 \rightarrow E_2 \rightarrow E_4$ process should reveal a quadratic dependence on the input intensity. Since our photovoltage spectra were measured with a Fourier transform infrared spectrometer, this effect translates into a peak proportional to $I_{\rm in}^2$ at the second harmonic frequency.

We first verified that the transition energy $E_1 \rightarrow E_4$ is indeed twice as large as the energy difference between E_1 and E_2 by measuring both optical absorption of the white light source at this wavelength and photodetection of a 780 nm laser diode. We then inspected the nonlinear response of our material under white light illumination at various input intensity levels. In the spectral response, we consistently observe a peak around 6500 cm^{-1} and a second harmonic peak at 13 000 cm^{-1}. As shown in Fig. 4(a), the signal size of the second harmonic peak $S_{2\omega}$ as a function of the signal size at the fundamental frequency S_ω follows a parabola as described by the equation $S_{2\omega}(S_\omega)=aS_\omega^2$. This quadratic dependence of the second harmonic signal is a quite strong argument to prove the existence of a noncoherent, resonant two-photon process. In order to exclude trivial effects, like for instance device heating, at the origin of the nonlinearity, we conducted a second experiment at a range of much higher input intensities. In this case, the light source was a 1.55 μm laser diode operated up to an optical power of 50 mW and focused into a small spot of 10 μm diameter. We investigated the integrated signal strength at the fundamental frequency S_ω as a function of laser injection current I. Instead of the linear signal increase seen in the low intensity experiment, we observe a saturation behavior which is very well fitted by a parabola [see Fig. 4(b)]. The strong deviation from linearity observed at higher input intensity is the result of two related effects: electrons excited from E_2 to E_4 reduce the size of the OR signal in the $E_1 \rightarrow E_2$ transition, but they also increase the signal size of the $E_2 \rightarrow E_4$ transition. Since the two transitions involve electron displacements into opposite directions, the decreasing electron density in level E_2 along with the increasing electron density in level E_4 result in the same overall effect: The signal at the fundamental frequency will exhibit a quadratic saturation behavior according to $S_\omega(I)=a(I-I_{\rm th})-b(I-I_{\rm th})^2$. Although at this point only a qualitative agreement between theory and experiment is demonstrated, we have found clear evidence for a resonant, noncoherent two-photon process in GaN/AlN QWs. Together with a recently published work on second harmonic generation in GaN/AlN QWs,[14] our results indicate a considerable application potential for such short period superlattice structures in the area of NLO frequency conversion.

This work was financially supported by the Professorship Program and the National Center of Competence in Research "Quantum Photonics" sponsored by the Swiss National Science Foundation and by the European Commission via the Strep "Nitwave" (contract #004170).

[1] J. A. Giordmaine, Phys. Today **22**(1), 39 (1969).
[2] see http://www.wickedlasers.com/Green_Lasers-3-1.html
[3] H. P. Weber, J. Appl. Phys. **38**, 2231 (1967).
[4] M. Bass, P. A. Franken, J. F. Ward, and G. Weinreich, Phys. Rev. Lett. **9**, 446 (1962).
[5] E. Rosencher, Ph. Bois, B. Vinter, J. Nagle, and D. Kaplan, Appl. Phys. Lett. **56**, 1822 (1990).
[6] E. Rosencher, P. Bois, J. Nagle, E. Costard, and S. Delaitre, Appl. Phys. Lett. **55**, 1597 (1989).
[7] C. Gmachl, H. M. Ng, S. N. G. Chu, and A. Y. Cho, Appl. Phys. Lett. **77**, 3722 (2000).
[8] N. Suzuki and N. Iizuka, Jpn. J. Appl. Phys., Part 2 **36**, L1006 (1997).
[9] N. Iizuka, K. Kaneko, and N. Suzuki, Appl. Phys. Lett. **81**, 1803 (2002).
[10] D. Hofstetter, S.-S. Schad, H. Wu, W. J. Schaff, and L. F. Eastman, Appl. Phys. Lett. **83**, 572 (2003).
[11] F. R. Giorgetta, E. Baumann, F. Guillot, E. Monroy, and D. Hofstetter, Electron. Lett. **43**, 185 (2007).
[12] O. Ambacher, J. Smart, J. R. Shealy, N. G. Weimann, K. Chu, M. Murphy, W. J. Schaff, L. F. Eastman, R. Dimitrov, L. Wittmer, M. Stutzmann, W. Rieger, and J. Hilsenbeck, J. Appl. Phys. **85**, 3222 (1999).
[13] E. Rosencher and Ph. Bois, Phys. Rev. B **44**, 11315 (1991).
[14] L. Nevou, M. Tchernycheva, F. Julien, H. Raybaut, A. Godard, E. Rosencher, F. Guillot, and E. Monroy, Appl. Phys. Lett. **89**, 151101 (2006).